

Targeted mRNA degradation by complex-mediated delivery of antisense RNAs to intracellular human mitochondria

Saikat Mukherjee, Bidesh Mahata[†], Biraj Mahato and Samit Adhya*

Genetic Engineering Laboratory, Indian Institute of Chemical Biology, 4 Raja S. C. Mullick Road, Calcutta 700032, India

Received November 27, 2007; Revised and Accepted January 16, 2008

Mitochondrial dysfunction underlies a large number of acute or progressive diseases, as well as aging. However, proposed therapies for mitochondrial mutations suffer from poor transformation of mitochondria with exogenous DNA, or lack of functionality of the transferred nucleic acid within the organelle. We show that a transfer RNA import complex (RIC) from the parasitic protozoan *Leishmania tropica* rapidly and efficiently delivered signal-tagged antisense (STAS) RNA or DNA to mitochondria of cultured human cells. STAS-induced specific degradation of the targeted mitochondrial mRNA, with downstream effects on respiration. These results reveal the existence of a novel small RNA-mediated mRNA degradation pathway in mammalian mitochondria, and suggest that RIC-mediated delivery could be used to target therapeutic RNAs to the organelle within intact cells.

INTRODUCTION

The critical role of mitochondria in the etiology of a variety of inherited and complex disorders, and of aging, is well established (1–5). Point mutations and deletions of mitochondrial DNA (mtDNA) cause acute or progressive encephalomyopathies for which therapies have been proposed but not proved (6). At the same time, genetic analysis of mitochondrial replication and gene expression is hampered by the lack of an efficient gene transduction system.

The major problem is that mammalian mitochondria, with their double membrane envelope, are resistant to transfection with DNA by conventional techniques. Human mitochondria have been reported to be naturally competent (7), but the nature of this competence is unknown, and we have not observed any significant unassisted uptake of RNA into human mitochondria *in vitro* (see in what follows). DNA was introduced into isolated mitochondria by electroporation (8), but in the absence of a demonstration of its efficacy on intracellular mitochondria, the genetic or therapeutic potential of electroporation is limited. DNA conjugated to a mitochondrial signal peptide was imported via protein import channels into isolated mitochondria (9), but there are no reports of the effects of peptide-DNA conjugate on mitochondria within

intact cells. Peptide nucleic acids (PNAs) coupled to a lipophilic cation were taken up into the mitochondria of human cells; although PNA inhibited mutant DNA replication *in vitro*, it was without effect in intracellular mitochondria (10). Allotopic expression of a modified yeast tRNA gene in the nucleus resulted in partial correction of the respiratory defects of cells containing a mitochondrial tRNA^{Lys} mutation (11); since in this case biological activity depends upon the import into the mitochondria of tRNA of a single specificity (for lysine), its application is likely to be limited to only a few diseases affected by this mutation. For therapeutic application, high efficiency transfer, biological activity and general applicability are desirable attributes of any nucleic acid delivery system.

An alternative approach was suggested by our observation that a purified RNA Import Complex (RIC; 12) from the protozoal parasite *Leishmania tropica* is taken up and targeted in a biologically active form to mitochondria of primary and cultured mammalian cells through a caveolin-1-dependent (i.e. endocytotic) pathway (13). Mitochondrion-localized RIC induced import of several endogenous cytosolic tRNAs, leading to correction of the respiration defect in intracellular mitochondria with the MERRF (Myoclonic epilepsy with

*To whom correspondence should be addressed. Tel: +91 3324733491; Fax: +91 3324735197; Email: sadhya@iicb.res.in

[†]Present address: Department of Pharmacology, University of Wisconsin, Madison, WI 53706, USA.

Ragged Red Fibers) mutation in the mitochondrial tRNA^{Lys} gene (13,14). Although RIC treatment would be useful in many diseases caused by different mitochondrial tRNA mutations [e.g. late onset Alzheimer's disease (tRNA^{Gln}) or Maternally Inherited Diabetes and Deafness (tRNA^{Leu})], it is not applicable to mutations or deletions in protein-coding genes.

RIC contains eight nucleus- and three mitochondrion-encoded subunits, six of which are essential for import activity (15). Through its largest subunit RIC1, the complex binds with nanomolar affinity to cognate tRNAs and to an oligoribonucleotide derived from the D arm of *Leishmania* tRNA^{Tyr} (GUA) and containing an import signal (16). In this report, we have examined whether these two properties of RIC, i.e. intracellular targeting and high affinity for RNA, can be combined to achieve mitochondrial delivery of functional RNA.

RESULTS

Targeting strategy

To examine the ability of RIC to deliver functional RNAs, several RNA oligomers (Signal-Tagged AntiSense or STAS) were synthesized, each of length ~40 nt, with (i) an import signal corresponding to the D arm hairpin of *Leishmania* tRNA^{Tyr} (16) at its 5' end, followed by (ii) a gene-specific antisense sequence complementary to the 5'-terminal region (spanning the first 5–6 codons) of a mitochondrial mRNA (Fig. 1A, Supplementary Material, Fig. S1). The tagged RNA would bind RIC through the import signal and be ferried to mitochondria, the ultimate destination of RIC in its internalization pathway (13). Within the organelle, the antisense moiety would bind to the initiation region of the target mRNA, leading to translation inhibition through steric exclusion of ribosomes and/or initiation factors. In order to test the generality of the approach, mitochondrion-encoded subunits of various respiratory complexes were targeted: ND1 of complex I (NADH dehydrogenase); CYB of complex III (ubiquinol–cytochrome *c* reductase); COI and COII of complex IV (cytochrome *c* oxidase); and A6 of complex V (F1Fo-ATP synthase).

Uptake of signal-tagged RNAs by isolated and intracellular mitochondria

Initially, we checked the suitability of STAS RNAs as import substrates of RIC. Isolated mitochondria from HepG2 (human cell line) were pre-incubated with purified RIC to make them import-competent, as shown previously (14). The import of radiolabeled RNAs into the RIC-reconstituted mitochondria was assayed by RNase protection. In the presence of RIC, all the STAS RNAs tested were imported. Import was dependent on RIC, as well as on the signal tag, since AS(ND1), targeted to the ND1 mRNA but lacking the D arm hairpin, was not imported (Fig. 1B).

Cross-linking of RIC with the D arm hairpin does not affect uptake and mitochondrial targeting of the complex but inhibits import of the covalently bound RNA (13). Thus the two functions of RIC—targeting and import—function independently, suggesting the possibility of using RIC as a carrier for

mitochondrial delivery of exogenous signal-tagged import substrates. To examine the uptake of these RNAs by intact cells, Alexa Fluor 488-labeled untagged or tagged STAS RNAs were pre-incubated with purified RIC and the noncovalent RNA-protein complex administered to monolayers of the hepatocarcinoma cell line HepG2. Mitochondrial localization in live cells was monitored by staining with the marker dye MitoTracker Deep Red 633. After 1 h of incubation, STAS RNA targeting the mRNA encoding the ND1 subunit of respiratory complex I [STAS(ND1)] was detected as discrete spots on the cell surface. The size, shape and distribution of these regions of local RNA concentration are similar to the discrete spots of RIC previously detected at early times on the same cells or in caveolin-1 downregulated HepG2 (13), and presumably represent the receptor-bound RNA–RIC complex. Internalization and mitochondrial localization of the RNA was evident by 3 h. By 24 h, the RNA was localized in most of the mitochondria in ~85% of the treated cells (Fig. 1D,F). There was no uptake of AS(ND1), or of STAS(ND1) in the absence of RIC, but the signal tag alone (D) was taken up normally, as expected (Fig. 1E). These experiments illustrate the rapid and quantitative uptake and targeting of signal-tagged RNAs mediated by RIC.

The ability of this system to transport and target signal-tagged DNA oligonucleotides was also examined. For this purpose, an RNA–DNA chimera was prepared, containing the D arm RNA hairpin at the 5' end covalently linked to the ND1 antisense (DNA) sequence. The intact chimera was efficiently imported into isolated mitochondria, and was recovered from the mitochondrial fraction of treated cells (Fig. 1C). The imported species was sensitive to both DNase and RNase; RNase treatment resulted in the removal of the hairpin from the DNA, as expected (Fig. 1C). A small fraction of the internalized chimera was in the post-mitochondrial fraction, i.e. soluble, vesicular or ribosome-bound form (Fig. 1C).

Specific degradation of target mRNAs induced by STAS

To check the effect of STAS on mitochondrial mRNAs, northern blots from STAS-treated cells were analyzed. More than 80% reduction of the targeted mRNA level was observed with different STAS RNAs (Fig. 2A, Supplementary Material, Table S1). Downregulation was specific for the target. For example, the level of ND1 mRNA was unaffected in the presence of STAS(COI), and vice versa, while COII mRNA was unaltered in STAS(CYB)-targeted mitochondria (Fig. 2A). Cytosolic mRNAs such as actin were not altered in STAS-treated cells (Fig. 2B). These experiments show the existence of a degradation mechanism that recognizes targeted double-stranded RNA regions on mitochondrial mRNAs.

Although targeting was mRNA-specific, the presence of a single base insertion [in STAS(ND1)] or 1–3 mismatches with the target [STAS(ND1-1,2 and 3; Fig. 1A)] did not substantially affect downregulation (Fig. 2B). The tolerance of targeting to multiple mismatches within the duplex is probably due to the high GC content and enhanced stability of the RNA:RNA helices.

STAS RNAs targeting the 5' terminus (starting at position 1 of the mRNA), the stop codon (position 943) and internal position 324 were effective, whereas one targeting position

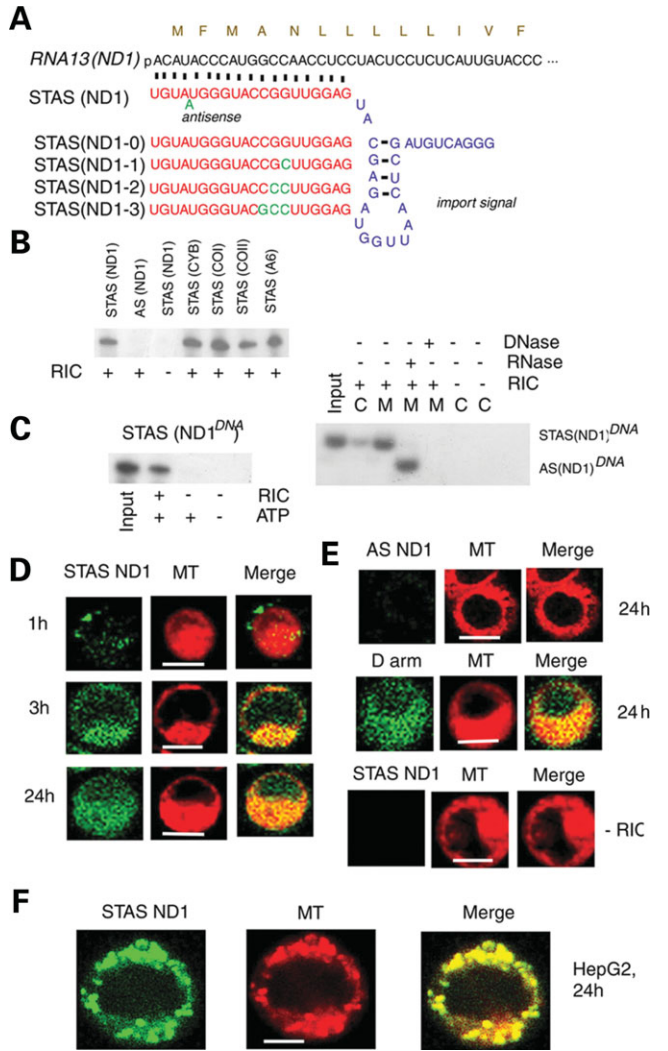


Figure 1. Uptake of signal-tagged antisense RNA (STAS) by mammalian cells and tissues. (A) Molecular design of STAS. Each STAS molecule is a chimera of a 5' import signal (the D arm hairpin of *Leishmania* tRNA^{Tyr}(GUA); blue) and a 3' RNA sequence (red) complementary to the 5'-translation initiation region of the target mRNA. For illustration, targeting of *RNA 13*, encoding the NADH dehydrogenase subunit 1 (ND1) is shown; other targeting events are shown in Supplementary Material, Fig. S1. Anti-ND1 sequences with 0–3 mismatches with the target (green) are shown. (B) Import of STAS RNAs targeting various mt mRNAs into HepG2 mitochondria. Cells were cultured for 48 h with the indicated combinations of RIC and ³²P-labeled STAS RNA, then mitochondria were isolated and mtRNA analyzed by autoradiography. CYB, apocytochrome b; COI, COII, cytochrome oxidase subunits I and II; A6, F1Fo ATP synthase subunit 6. (C) Left, import of ³²P-labeled STAS RNA–DNA chimera [STAS(ND1)^{DNA}] into isolated mitochondria in the presence or absence of RIC and ATP. Right, RIC-dependent uptake of ³²P-labeled STAS chimera by HepG2 cells in the presence or absence of RIC and their localization in the mitochondrial (M) or cytosolic (C) fraction. The recovered RNA was treated with DNase or RNase and rerun in parallel. The labeled RNase-resistant fragment is the *in vitro* synthesized oligomer primed by D arm RNA of low specific activity. (D) Confocal images of live HepG2 cells treated with RIC and Alexa Fluor-labeled STAS(ND1) RNA (green) for the indicated times. Cells were counterstained with Mitotracker Deep Red 633 (red). Bar, 15 μm. (E) Dependence of STAS uptake on import signal and RIC. Indicated RNAs were incubated with HepG2 cells for 24 h in the presence (top and middle) or absence (bottom) of RIC. (F) Higher magnification of a Hep G2 cell treated with STAS(ND1). Bar, 6.9 μm.

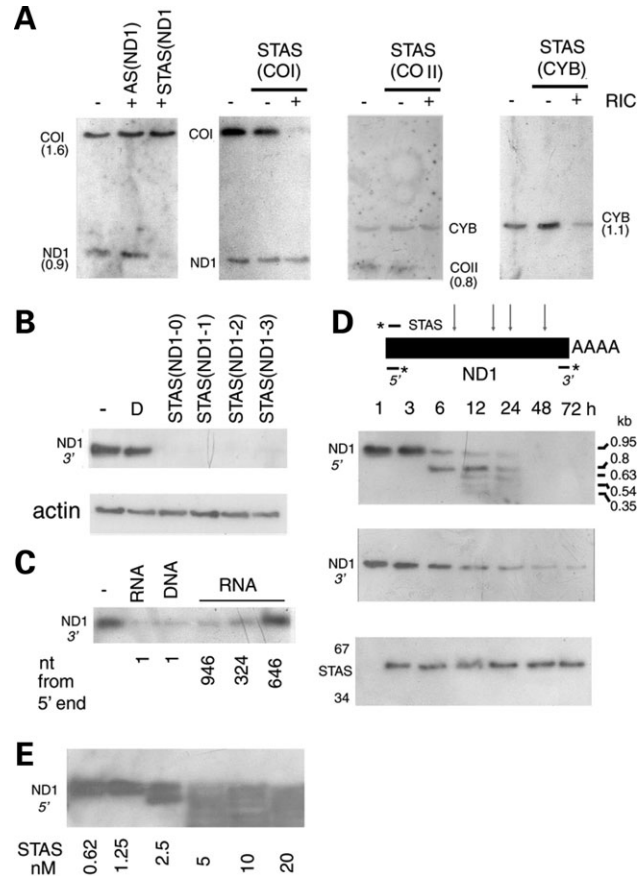


Figure 2. Fate of STAS-targeted mitochondrial mRNAs. (A) Northern blots of mitochondrial RNA from Hep G2 cells treated for 48 h with the STAS RNAs indicated at the top, probed with oligonucleotides complementary to the mt genes indicated next to each band. In the leftward three panels, the blot was sequentially hybridized with the probes indicated. Sizes (kb) of the respective mRNAs (27) are indicated. (B and C) Effect of STAS-target mismatch (B) and position (C) on ND1 mRNA. HepG2 cells were treated with the indicated RNAs and mitochondrial ND1, or cytosolic β-actin, mRNA probed after 48 h. D, D arm RNA; STAS(ND1-0,1,2,3), signal-tagged RNA with 0–3 mismatches with target (Fig. 1A); DNA, signal-tagged anti-ND1 oligodeoxynucleotide; starting positions of ND1 mRNA targeted are indicated below panel C. (D) Time-dependent degradation of STAS-targeted ND1 mRNA. Northern blots of mt mRNA from Hep G2 cells treated with STAS(ND1)-RIC for the indicated times. Probes: top, ND1 5' (antisense); middle, ND1 3' (antisense); bottom, ND1 5' (sense). Positions of the probes on the mRNA map, and degradation pause sites (arrows), are shown at the top. (E) Dose-dependence of STAS-induced target degradation. Cells were treated with the indicated concentrations of STAS(ND1) plus RIC for 12 h.

646 was not (Fig. 2C); degradation could be influenced by structural features of the mRNA denying or facilitating access to the antisense probe.

In addition to RNA, chimeras of single-stranded DNA oligonucleotides covalently attached to D arm RNA, were taken up into isolated as well as cellular mitochondria (Fig. 1C), and induced degradation of the target mRNA (Fig. 2C). This implies that the degradation mechanism recognizes both RNA:RNA duplexes and RNA:DNA hybrids.

Time course experiments were performed to compare the uptake of STAS with the degradation of the target mRNA

by northern blotting. Essentially complete mitochondrial uptake of STAS(ND1) RNA occurred rapidly, between 1 and 3 h; the imported RNA persisted at peak level for at least 72 h (Fig. 2D). The kinetic data confirm the microscopic uptake studies showing mitochondrial targeting within 3 h of treatment (Fig. 1). Moreover, they indicate the high stability (half-life in excess of 3d) of the internalized STAS.

The level of the target mRNA was unchanged up to 3 h; from 6 h onwards, a series of partial degradation products appeared, leading to the complete disappearance of hybridizable mRNA by 48 h (Fig. 2D). In this experiment, the probe hybridizing with the degradation products is complementary to the 5' terminal sequence of the target; in contrast, only the full-length mRNA hybridized with an oligonucleotide complementary to the 3'-end of the coding region (Fig. 2D). Thus the partial products represent pause sites of the degradation machinery at various distances from the 5' end.

The effect of STAS dosage on its biological effect (target degradation) on cultured cells was studied. In 12 h-treated cells, degradation of the target was evident between 2.5 and 5 nM STAS (Fig. 2E). A further increase in STAS concentration in the culture medium did not lead to enhancement of degradation rate, since identical degradation patterns were observed between 5 and 20 nM (Fig. 2E). Thus, target sites are saturated within ~ 5 nM STAS, with excess antisense RNA having no effect on degradation rate.

STAS-mediated inhibition of cellular respiration

The downstream effects of STAS-induced downregulation of mitochondrial mRNAs on cellular respiratory functions were examined. In mitochondria from STAS-treated cells, synthesis of the targeted protein was specifically reduced, with no significant effect on the rest of the mitochondrial proteome (Fig. 3A). Significant downregulation occurred with all the antisense RNAs tested, although the extent of inhibition was somewhat variable after 48 h of treatment, with marked effects with a few, e.g. anti-CYB and anti-ND1. In all cases, the translation initiation region was targeted; thus, the variability may be a result of structural features of the mRNAs that preclude or enhance binding of the antisense RNA.

To test whether the observed downregulation of target protein synthesis was sufficient to inactivate the corresponding respiratory complex, activity assays of these complexes in inner membrane extracts, or *in situ*, were performed. In STAS(ND1)-treated cells, the activity of NADH dehydrogenase (complex I) was reduced by more than 80%; in the same cells, the activities of other respiratory complexes were unaffected (Fig. 3B; Supplementary Material, Tables S2–S4). Similarly, complex III activity was undetectable, but complex I activity normal, in the presence of STAS(CYB), while cytochrome *c* oxidase activity was specifically affected in cells treated with anti-COI (Supplementary Material, Tables S2–S4).

Thus the path of electrons from respiratory substrates to molecular O₂ could be blocked at different steps of the electron transport chain. This was reflected in a ~ 4 -fold reduction in O₂ uptake by cells targeted at ND1 (complex I), CYB (complex III) and COI (complex IV) (Fig. 3C). Neither RIC alone, nor the import signal in the presence of RIC, affected

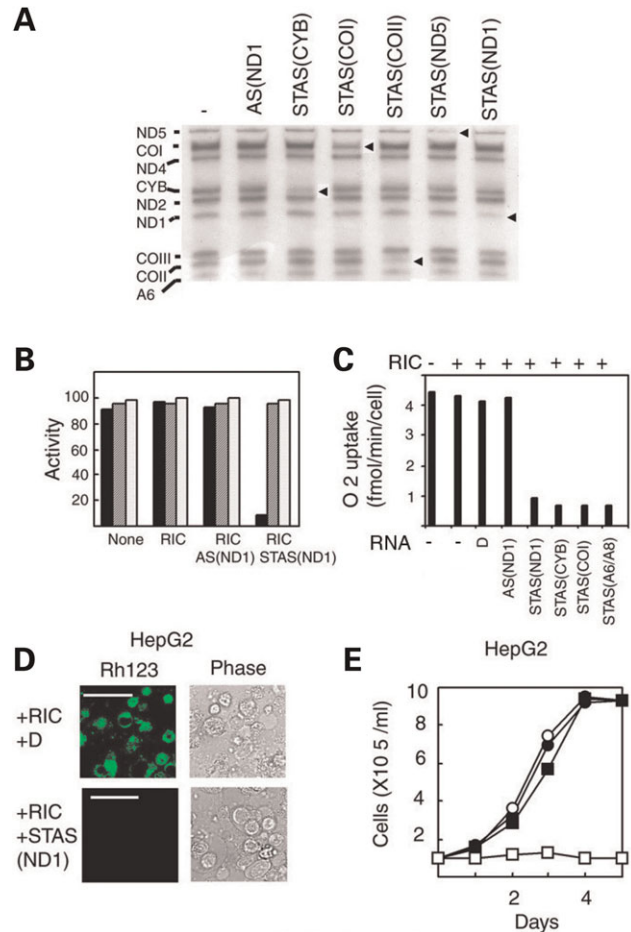


Figure 3. Biochemical and physiological effects of STAS RNA. (A) Synthesis of ³⁵S-methionine-labeled proteins in mitochondria from Hep G2 cells treated with RIC and the indicated RNAs. Individual downregulated proteins are indicated by arrowheads. Mitochondrion-encoded protein bands identified at the left. (B) Mitochondrial NADH dehydrogenase (complex I) activity (black bars) in Hep G2 cells treated with the indicated RNAs for 2d. The same mitochondrial extracts were assayed for complex III (hatched bars), and the cells stained for cytochrome *c* oxidase (complex IV; stippled bars). (C) Oxygen uptake in 48 h STAS-RIC treated Hep G2 cells. Additions to the culture were as indicated. In (B) and (C), activities are expressed as percent maximum. Mean values and standard deviations are shown in Supplementary Material, Tables S2–S5. (D) Hep G2 cells were treated with RIC, along with D arm RNA (upper) or STAS(ND1) (lower) for 48 h, and live cells were stained with rhodamine 123. Bar, 30 μ m. (E) Growth of Hep G2 cells treated with RIC and D arm RNA (circles) or STAS(ND1) (squares) in glucose-deficient DMEM medium supplemented with glucose (open symbols) or galactose (filled symbols).

respiration (Fig. 3C). In parallel, the uptake of rhodamine 123, a membrane potential-sensitive dye that is concentrated by actively respiring mitochondria (17), was significantly reduced (Fig. 3D). The quantified rhodamine 123 fluorescence in individual cells was lowered by $\sim 70\%$ from 75.2 ± 5.2 ($n = 50$) to 22.7 ± 6.2 ($n = 50$) arbitrary units/cell for untreated and STAS(ND1)-treated HepG2, respectively. A similar reduction [to 28.0 ± 2.6 ($n = 17$) units/cell], but not elimination, of rhodamine 123 uptake was also observed in the cybrid FLP32.39, containing a mitochondrial deletion of four genes including those encoding two cytochrome *c*

oxidase subunits (18). The residual membrane potential in these respiration-deficient cells is probably created by complex V-mediated hydrolysis of glycolytically generated ATP. The lowering of the membrane potential is due to inhibition of the transmembrane proton gradient, the formation of which is coupled to electron transport. Inhibition of ATP synthesis by antisense-mediated downregulation of subunit A6/A8 (both subunits are translated from the same mRNA), also resulted in inhibition of O₂ uptake by 85% (Fig. 3C); this reflects the two-way coupling between the proton gradient and ATP synthesis in these antisense-transformed mitochondria. In cybrids homoplasmic for a mutation in the A6 gene, as well as normal cells treated with oligomycin (a complex V inhibitor), the inhibition of O₂ uptake is more moderate, about 50–60% (19). The similar extents of acute inhibition of respiration (~85%) in all the antisense transformants could be due to a generalized damage of respiratory complexes, e.g. by accumulation of Reactive Oxygen Species (ROS), which has been shown to occur in the A6 mutant cybrids (19).

In spite of the respiratory deficiency, mitochondrial antisense-transformed cells grew normally in glucose-containing media, presumably depending upon glycolysis to generate ATP (Fig. 3E). Failure to utilize galactose is a characteristic of respiration-deficient cells (20). In normal, glucose-containing medium, STAS(ND1) had no appreciable effect on the growth or morphology of the hepatocarcinoma (Hep G2) cells; however, in the presence of galactose, STAS(ND1)-treated HepG2 cells were unable to grow (Fig. 2E).

DISCUSSION

In this report we show that the protozoal RNA transporter RIC delivers signal-tagged exogenous small RNA or DNA into mitochondria of cultured human cells. Delivery is highly efficient: RNA is transferred to most or all of the mitochondria in more than 80% of the cells within 3 h of treatment (Fig. 1). The imported RNA is stable, with a half-life of greater than 3d (Fig. 2). Moreover, antisense sequences appended to the tag induce specific and quantitative degradation of the corresponding mRNA (Fig. 2). This procedure requires the application of nanomolar quantities of RNA, is generally applicable to multiple mitochondrial mRNAs and produces predictable effects on cellular respiration. It will be pertinent here to compare this delivery method to existing methods of gene transfer.

Among the existing physical, chemical and biological methods of gene transfer, the one with the closest similarity to the complex-mediated transfer described here uses viral vectors (21). Both viruses and RIC deliver DNA or RNA with high efficiency to intact cells. Most viruses are taken up endocytotically, utilizing specific cell-surface receptors; RIC is similarly internalized by a caveolin-dependent, presumably endocytotic pathway (13). However, whereas the viral genome is targeted to the nucleus or retained in the cytosol, signal-tagged nucleic acids are targeted to mitochondria by RIC. The exploitation of cell surface receptors and intracellular trafficking pathways accounts for the high efficiency of

both viral and RIC-mediated gene transfer. Viral capsids enclose and protect the genomic cargo, and can deliver several kilobases of DNA/RNA; in contrast, the ability of RIC to carry small RNA oligonucleotides has been demonstrated, and the cargo is bound to the protein complex but may be significantly exposed to the medium. The rapid uptake of RIC-bound RNA may minimize extracellular degradation; inside the organelle, the RNA is remarkably stable, most likely due to the presence of the D arm hairpin at the 5' end.

Antisense Oligonucleotides (ASO) and double-stranded small interfering (si) RNAs have been employed to target cellular and viral mRNAs *in vivo*, and some are under clinical trial or have been approved for therapeutic application (22). Current protocols use chemically modified oligonucleotides for enhanced stability and targeting specificity. However, the uptake mechanism is unknown, and delivery is slow and inefficient, requiring high concentrations (>100 nM) of ASO. Moreover, short hairpin RNAs, which generate siRNAs intracellularly, have been reported to have *in vivo* toxicity (23). In contrast, RIC delivers unmodified RNA rapidly and efficiently to the targeted compartment. RIC is known not to have any significant cytotoxic effects on cultured cells (13), but the efficacy and toxicity of RIC-mediated procedures in animal models are yet to be evaluated.

A number of approaches to deliver nucleic acids to mitochondria have been reported. Oligonucleotides coupled to a mitochondrial targeting peptide (9) and PNAs conjugated with lipophilic cations (10) are technically demanding and expensive to prepare, in comparison to the use of simple unmodified RNA/DNA in the RIC method. Moreover, the problems of targeting efficiency and biological efficacy associated with these approaches are largely absent in the current procedure.

Not much is known about post-transcriptional regulatory mechanisms in mitochondria (24). Our experiments reveal for the first time the existence of a mitochondrial pathway for small RNA-mediated degradation of mRNA. Degradation is target-specific, presumably signaled by the pairing of the antisense with its target site, but the efficiency may vary between targets or between different sites within the same mRNA. In prokaryotes (from whose ancestors mitochondria were presumably derived), a number of small RNAs regulate target mRNAs post-transcriptionally under stress conditions (25). In these systems, mRNA degradation involves the degradosome, a complex of proteins including an RNA helicase, an RNase III-type endonuclease and an exonuclease (25). Yeast mitochondria contain a similar complex (26), and mammalian mitochondria contain a helicase (Suv3p) (27) and an exonuclease (polynucleotide phosphorylase) (28). The roles of these proteins in antisense-mediated mRNA degradation remain to be elucidated. Interestingly, human Suv3p acts on both RNA:RNA and RNA:DNA duplexes (27); the degradative effect of tagged RNA or DNA (Fig. 2) may be the reflection of the involvement of this protein. It will be important to determine whether the degradosome is involved in antisense-mediated mRNA degradation, and whether this mechanism has any physiological significance in terms of regulating mitochondrial function.

MATERIALS AND METHODS

Cell culture

The human hepatocarcinoma cell line HepG2 was cultured as monolayers in DMEM medium containing 4.5 g/l glucose, 110 mg/l sodium pyruvate and 10% fetal bovine serum (FBS). Growth of HepG2 cells was monitored on glucose-deficient DMEM supplemented with 0.9 mg/ml of glucose or galactose.

Preparation of signal-tagged RNAs

Signal-tagged antisense (STAS) RNAs consisted of a 5' domain containing the D arm hairpin from *L. tropica* and a 3' domain complementary to a specific targeted mitochondrial mRNA (Supplementary Material, Table S6). Target design was based on the published human mitochondrial genome sequence (29). Appropriate oligonucleotide templates were prepared and transcribed with T7 RNA polymerase (Supplementary Materials). To prepare fluorescent RNA, the transcription reaction contained, additionally, 0.5 nmol of 5-Alexa Fluor 488-UTP (Molecular Probes).

Preparation of signal-tagged DNA

D arm RNA was synthesized as described (30), and 10 pmol was annealed to 50 pmol of the anti-ND1 oligonucleotide O-284 (Supplementary Material, Table S6). The RNA primer was extended with Klenow enzyme in the presence of the four dNTPs including [α - 32 P] TTP, to yield the RNA–DNA chimera which was melted off and gel-purified. The product was further confirmed to be the expected RNA–DNA adduct by treating one fraction with RNase A plus T1 for 15 min at 37°C and another with 1.5 units of DNase I for 20 min on ice, and running the digests on a 6% denaturing PAGE.

Purification of RIC

RIC was purified from inner membrane extracts of *L. tropica* by RNA affinity chromatography (12).

Mitochondrial import assay

HepG2 mitochondria (100 μ g protein), isolated as described (31), were pre-incubated for 1 h on ice with RIC (200 ng), then incubated with 2.5 nM of 32 P-labeled RNA in import buffer in the presence of 4 mM ATP at 37°C for 15 min, and RNase-resistant imported RNA analyzed by gel electrophoresis (14).

Treatment of cells with antisense RNA

RNA and RIC (200 ng) were pre-incubated in 20 μ l of buffer BB (10 mM Tris–HCl, pH 7.5, 10 mM MgCl₂, 1 mM DTT) for 30 min at 4°C, to allow complex formation. The mixture was then directly applied to ~1 ml medium over HepG2 monolayers in 40-mm diameter Petri dishes and the cells cultured for the indicated times before harvesting.

Northern analysis

Mitochondria were isolated from lysates of STAS-treated cells by differential centrifugation, and treated with 2.5 μ g/ml of RNase A and 50 units/ml of RNase T1 for 15 min at 37°C. RNA was prepared by guanidinium isothiocyanate extraction and run on 1% agarose-formaldehyde gels in 0.2 M MOPS, 50 mM sodium acetate, 1 mM EDTA, transferred to Hybond N⁺ membrane (Amersham-GE) by semi-dry transfer, and UV-crosslinked to the membrane. Blots were pre-hybridized for 4–6 h at 50°C in OH buffer: 5XNET (0.5 M NaCl, 0.1 M Tris–HCl, pH 7.5, 5 mM EDTA), 5X Denhardt's solution (0.5% bovine serum albumin, 0.5% Ficoll, 0.5% polyvinyl pyrrolidone), 20 mM sodium phosphate, 0.1% SDS and 200 μ g/ml denatured calf thymus DNA. The filters were hybridized at 50°C overnight with 5'– 32 P labeled oligonucleotide probe (10⁵–10⁶ cpm/ml) in buffer OH. Blots were given stringency washes: 6XSSC, 0.1% SDS, room temperature, thrice; and 6XSSC, 0.1% SDS, 65°C, once. Washed membranes were autoradiographed. In some cases, a blot was sequentially hybridized with two probes without an intervening melt-off step, so that mRNAs of different sizes could be simultaneously visualized.

Assays of mitochondrial function

In organello translation, respiratory complex activity and O₂ uptake assays were performed as described (Supplementary Material).

Live cell imaging

HepG2 monolayers were harvested, washed with PBS-glucose at 4°C, and allowed to adhere to polylysine-coated slides. Adhered cells were overlaid with staining solution, and after 5–15 min, were observed under a Leica DMIRB confocal microscope. Staining solutions contained PBS-glucose and Mitotracker Deep Red (1 μ M) or Rhodamine 123 (0.2 μ g/ml). Illumination laser wavelengths were 488 nm (Alexa Fluor 488 and Rhodamine 123) and 633 nm (Mitotracker Deep Red). Control and experimental specimens were scanned and analyzed under identical gain and other settings. Image capture, processing and quantification of fluorescence were carried out using Leica SP2 confocal software.

SUPPLEMENTARY MATERIAL

Supplementary Material is available at HMG Online.

ACKNOWLEDGEMENTS

We thank Gayatri Tripathi and Tapas Chowdhury for technical assistance.

Conflict of Interest statement. None declared.

FUNDING

Supported by DST grant #SR/SO/BB-28/2003 (to S.A.), CSIR project #SIP 0007 and CSIR Research Fellowships to S.M., Bidesh Mahata and Biraj Mahata.

REFERENCES

- Taylor, W.R. and Turnbull, D.M. (2005) Mitochondrial DNA mutations in human disease. *Nat. Rev. Genet.*, **6**, 389–402.
- Lane, N. (2006) Powerhouse of disease. *Nature*, **440**, 600–602.
- Gottlieb, E. and Tomlinson, I.P.M. (2005) Mitochondrial tumor suppressors: a genetic and biochemical update. *Nat. Rev. Cancer*, **5**, 857–866.
- Lowell, B.B. and Shulman, G.I. (2005) Mitochondrial dysfunction and Type 2 diabetes. *Science*, **307**, 384–387.
- Balaban, R.S., Nemoto, S. and Finkel, T. (2005) Mitochondria, oxidants, and aging. *Cell*, **120**, 483–495.
- Gardner, J.L., Craven, L., Turnbull, D.M. and Taylor, R.W. (2007) Experimental strategies towards treating mitochondrial DNA disorders. *Biosci. Rep.*, **27**, 139–150.
- Koulintchenko, M., Tamperley, R.J., Mason, P., Dietrich, A. and Lightowlers, R.N. (2006) Natural competence of human mitochondria allows the molecular investigation of mitochondrial gene expression. *Hum. Mol. Genet.*, **15**, 143–154.
- Collombet, J.M., Wheeler, V.C., Vogel, F. and Coutelle, C. (1997) Introduction of plasmid DNA into isolated mitochondria by electroporation. A novel approach toward gene correction for mitochondrial disorders. *J. Biol. Chem.*, **272**, 5342–5347.
- Vestweber, D. and Schatz, G. (1989) DNA-protein conjugates can enter mitochondria via the protein import pathway. *Nature*, **338**, 170–172.
- Muratovska, A., Tamperley, R., Mason, A., Dietrich, A. and Lightowlers, R.N. (2001) Targeting peptide nucleic acid (PNA) oligomers to mitochondria within cells by conjugation to lipophilic cations: implications for mitochondrial DNA replication, expression and disease. *Nucl. Acids Res.*, **29**, 1852–1863.
- Kolesnikova, O., Entelis, N., Jacquis-Becker, C., Goltzene, F., Chrzanoska-Lightowlers, Z., Lightowler, R.N., Martin, R. and Tarassov, I. (2004) Nuclear DNA-encoded tRNAs targeted into mitochondria can rescue a mitochondrial DNA mutation associated with the MERRF syndrome in cultured human cells. *Hum. Mol. Genet.*, **13**, 2519–2534.
- Bhattacharya, S.N., Chatterjee, S., Goswami, S., Tripathi, G., Dey, S.N. and Adhya, S. (2003) ‘Ping pong’ interactions between mitochondrial tRNA import receptors within a multiprotein complex. *Mol. Cell. Biol.*, **23**, 5217–5224.
- Mahata, B., Mukherjee, S., Mishra, S., Bandyopadhyay, A. and Adhya, S. (2006) Functional delivery of a cytosolic tRNA into mutant mitochondria of human cells. *Science*, **314**, 471–474.
- Mahata, B., Bhattacharyya, S.N., Mukherjee, S. and Adhya, S. (2005) Correction of translational defects in patient-derived mutant mitochondria by complex-mediated import of a cytoplasmic tRNA. *J. Biol. Chem.*, **280**, 5141–5144.
- Mukherjee, S., Basu, S., Home, P., Dhar, G. and Adhya, S. (2007) Necessary and sufficient factors for import of tRNA into the kinetoplast-mitochondrion. *EMBO Rep.*, **8**, 589–595.
- Goswami, S., Dhar, G., Mukherjee, S., Mahata, B., Chatterjee, S., Home, P. and Adhya, S. (2006) A bi-functional tRNA import receptor from *Leishmania* mitochondria. *Proc. Natl Acad. Sci. USA*, **103**, 8354–8359.
- Chen, L.B. (1998) Mitochondrial membrane potential in living cells. *Annu. Rev. Cell Biol.*, **4**, 155–179.
- Sobreira, C., King, M.P., Davidson, M.M., Park, H., Koga, Y. and Miranda, A.F. (1999) Long-term analysis of differentiation in human myoblasts repopulated with mitochondria harboring mtDNA mutations. *Biochem. Biophys. Res. Comm.*, **266**, 179–186.
- Mattiazzi, M., Vijayvergia, C., Gajewski, C.D., DeVivo, D.C., Lenaz, G., Wiedmann, M. and Manfredi, G. (2004) The mtDNA T8993G (NARP) mutation results in an impairment of oxidative phosphorylation that can be improved by antioxidants. *Hum. Mol. Genet.*, **13**, 869–879.
- Hayashi, J., Ohta, S., Kikuchi, A., Takemitsu, M., Goto, Y. and Nonaka, I. (1991) Introduction of disease-related mitochondrial DNA deletions into Hela cells lacking mitochondrial DNA results in mitochondrial dysfunction. *Proc. Natl Acad. Sci. USA*, **88**, 10614–10618.
- Waeler, R., Russel, S. and Curiel, D. (2007) Engineering targeted viral vectors for gene therapy. *Nat. Rev. Genet.*, **8**, 573–587.
- Corey, D.R. (2007) RNA learns from antisense. *Nat. Chem. Biol.*, **3**, 8–11.
- Grimm, D., Streetz, K.L., Jopling, C.L., Storm, T.A., Pandey, K., Davis, C.R., Marion, P., Salazar, F. and Kay, M.A. (2006) Fatality in mice due to oversaturation of cellular microRNA/short hairpin RNA pathways. *Nature*, **441**, 537–541.
- Gagliardi, D., Stepien, P.P., Temperley, R.J., Lightowlers, R.N. and Chrzanoska-Lightowlers, Z.M.A. (2004) Messenger RNA stability in mitochondria: different means to an end. *Trends Genet.*, **20**, 260–267.
- Storz, G., Opdyke, J.A. and Zhang, A. (2004) Controlling mRNA stability and translation with small, noncoding RNAs. *Curr. Opin. Microbiol.*, **7**, 140–144.
- Dziembowski, A., Piwowarski, J., Hoser, R., Minczuk, M., Dmochowska, A., Siep, M., Spek, H., Grivell, L. and Stepien, P.P. (2003) The yeast mitochondrial degradosome. Its composition, interplay between RNA helicase and RNase activities and their role in mitochondrial degradosome. *J. Biol. Chem.*, **278**, 1603–1611.
- Minczuk, M., Piwowarski, J., Papworthy, M.A., Awiszuz, K., Schalinski, S., Dziebowski, A., Dmochowska, A., Bartnik, E., Tokatlidis, K., Stepien, P.P. and Borowski, P. (2002) Localization of the human hSuv3p helicase in the mitochondrial matrix and its preferential unwinding of dsDNA. *Nucl. Acid Res.*, **30**, 5074–5086.
- Piwowarski, J., Grzechnik, P., Dziembowski, A., Dmochowska, A., Minczuk, M. and Stepien, P.P. (2003) Human polynucleotide phosphorylase, hPNPase, is localized in mitochondria. *J. Mol. Biol.*, **329**, 853–857.
- Anderson, S., Bankier, A.T., Barrell, B.G., Bruijn, M.H.L., Coulson, A.R., Drouin, J., Eperon, I.C., Nierlich, D.P., Roe, B.A., Sanger, F. *et al.* (1981) Sequence and organization of the human mitochondrial genome. *Nature*, **290**, 457–464.
- Mahapatra, S., Ghosh, S., Bera, S.K., Ghosh, T., Das, A. and Adhya, S. (1998) The D arm of tRNA^{Lys} is necessary and sufficient for import into *Leishmania* mitochondria *in vitro*. *Nucl. Acids Res.*, **26**, 2037–2041.
- Enriquez, J.A. and Attardi, G. (1996) Analysis of aminoacylation of human mitochondrial tRNAs. *Meth. Enzymol.*, **264**, 183–196.